Long non-coding RNA XIST confers aggressive progression *via* miR-361-3p/STX17 in retinoblastoma cells

L.-L. YANG, Q. LI, X. ZHANG, T. CAO

Department of Ophthalmology, The Affiliated Hospital of Guizhou Medical University, Guiyang, Guizhou, China

Abstract. – **OBJECTIVE:** Retinoblastoma (RB) is a frequent intraocular tumor in children. Long-non-coding RNA X inactive specific transcript (XIST) has been reported to participate in the RB process, while its potential role remains largely unknown.

PATIENTS AND METHODS: The expression patterns of XIST, microRNA (miR)-361-3p, and Syntaxin 17 (STX17) were determined using quantitative Real Time-Polymerase Chain Reaction (qRT-PCR) assay. 3-(4,5-dimethyl-2-thiazolyl)-2,5-diphenyl-2-H-tetrazolium bromide (MTT), flow cytometry, and transwell assays were employed to reckon cell viability, apoptosis, and mobility in RB cells, respectively. Besides, the levels of STX17 and autophagy-related proteins were detected utilizing Western blot. Dual-Luciferase reporter assay was implemented to evaluate the interaction between miR-361-3p and XIST or STX17, and the role of XIST in tumor growth was analyzed through xenograft tumor model.

RESULTS: The expression levels of XIST and STX17 were higher in RB tissues and cells, but miR-361-3p was downregulated. Loss of XIST was inversely connected with aggressive characteristics, showing as the curb of cell proliferation, migration, invasion, autophagy, and enhancement of apoptosis in RB cells. Also, the deficiency of XIST caused the decrease of tumor growth in vivo. Meanwhile, miR-361-3p inhibitor partially rescued XIST detection-mediated cell behaviors *in vitro*. Similarly, miR-361-3p mimic-mediated suppressive effect on aggressive phenotypes was abolished after overexpression of STX17 in RB cells. Mechanically, XIST was a sponge of miR-361-3p to regulate STX17.

CONCLUSIONS: XIST functioned as an oncogenic lncRNA via miR-361-3p/STX17 axis in the progression of RB, which might provide a promising theoretical basis for the clinical therapy of RB.

Key Words:
    XIST, MiR-361-3p, STX17, RB.

Introduction

Retinoblastoma (RB) is a common intraocular tumor, and its most occurrence comes from children[1]. The incidence of RB is lower than that of other types of malignancy[2]. If the children with RB have entered an advanced stage, it means that there is a high chance of ocular extraction. Curative early diagnosis and therapy for RB appeared to be utterly critical[3,4]. To rescue the visual function of children, several therapeutic strategies have been operated and developed for varying degrees of RB[5]. According to the international classification of RB, it can be classified into A-E grades, and chemotherapy is successfully effective for the A-C group, but the ocular survival rate of grade D is only 10%-47% after systemic chemotherapy[6]. Furthermore, it is disappointing that the chemotherapy has little effectiveness on grade E patients[7,8]. Thus, novel therapeutic strategies are urgently required.

Long non-coding RNAs (lncRNAs) are a type of ncRNAs with over 200 nucleotides (nts) in length, accounting for 80% of ncRNAs[9-11]. LncRNAs are deemed to be strictly implicated in tumorigenesis[12], including RB[13]. Especially, Colon Cancer Associated Transcript-1 (CCAT1) serves as an oncogene in RB cells by inactivating microRNA (miRNA/miR)-218-5p[14]. X inactive specific transcript (XIST) is a better-known lncRNA, and it has been reported to be related to the pathogenesis of numerous human cancers. Interestingly, the role of XIST was inconsistent in different tumors. Especially, XIST functions as an oncogenic factor in osteosarcoma[15], but constrains aggressive cell phenotypes in breast cancer[16]. Besides, XIST has been demonstrated to expedite epithelial to mesenchymal transition (EMT) of RB *via*

Corresponding Author: Xi Zhang, MD; e-mail: yll147369@126.com

targeting miR-101[17]. Nevertheless, the potential regulatory mechanism of XIST in modifying RB needed to be further highlighted *in vitro* and *in vivo*.

One pivotal mechanism underlying the involvement of lncRNAs in mediating tumor growth was to modulate the expression of relevant miRNAs by acting as competitively endogenous RNAs (ceRNAs)[18]. For example, XIST contributes to the development of gastric cancer by sponging miR-185[19]. About miRNAs, they are defined according to the length (18-22 nts), and serve as master regulators, including oncogene and tumor suppressor, to regulate carcinogenesis and metastasis[20]. Several miRNAs have been identified to be implicated in RB progression. Chen et al[21] showed that miR-361-3p retards aggressive phenotypes (cell proliferation and metastasis) in non-small cell lung cancer. Additionally, microRNA-361-3p modulates cell proliferation by hedgehog signaling and functions as a tumor suppressor in RB[22]. Herein, we hypothesized that miR-361-3p could interact with XIST in monitoring tumor growth and metastasis of RB. Moreover, microRNAs mediate the expression of certain genes in multiple physiological and pathological processes[23]. Syntaxin 17 (STX17), as a Soluble NSF Attachment Protein Receptor (SNARE) of the autophagosome, is related to autophagy[24]. Whether STX17 could be implicated in miR-361-3p in mediating RB progression was the vital purpose of this present research.

In this paper, the expression profiles of XIST, miR-361-3p, and STX17 in RB tissues and cells were determined. Furthermore, the relationship between miR-361-3p and XIST or STX17 was also explained in subsequent assays.

Patients and Methods

Clinical Specimens and Cell Culture

The RB tissues (n=30) and matched non-tumor tissues (2 cm around tumors, n=30) were gained from enrolled patients who suffered from enucleation in the Affiliated Hospital of Guizhou Medical University. No participators had undergone other therapies before donation. Above all, written informed consents were gathered from each donator, and this research was approved by the Ethics Committee of the Affiliated Hospital of Guizhou Medical University.

For cell culture, RB cell lines (Y79 and WERI-Rb-1) and normal cell line (ARPE-19) were gained from Be Na Culture collection (Beijing, China). The above cells were cultured in Roswell Park Memorial Institute-1640 (RPMI-1640; Gibco, Grand Island, NY, USA) with 10% (for ARPE-19) or 20% (for Y79 and WERI-Rb-1) fetal bovine serum (FBS; Gibco, Waltham, MA, USA). Cells were placed in the conditions with 37°C and 5% CO_2.

Cell Transfection

Small interfering RNA (siRNA) and short hairpin (shRNA) against XIST (si-XIST and sh-XIST), their scrambles (si-NC and sh-NC), over-expression vector of STX17 (STX17) and STX17 blank control (pcDNA) were constructed in GenePharma (Shanghai, China). For oligonucleotides, miR-361-3p mimic, miR-361-3p inhibitor, and their controls (miR-NC and anti-miR-NC) were purchased from GenePharma (Shanghai, China). Then, transient transfection was performed using Lipofectamine 3000 (Invitrogen, Carlsbad, CA, USA) following the producer's description. Besides, sh-NC and sh-XIST were applied for setting up stably transfected cells with lentivirus-mediation.

Quantitative Real Time-Polymerase Chain Reaction (qRT-PCR) Assay

Total RNA was extracted and purified using TRIzol reagent (Invitrogen, Carlsbad, CA, USA) as per the manufacturer's manuals, and the harvested RNA maintained at -80°C until used. For the qRT-PCR assay, total RNA was subjected to reverse transcription (PrimeScript RT Reagent Kit; TaKaRa, Dalian, China) to obtain complementary DNA (cDNA). The formed cDNA was subjected to qRT-PCR utilizing the TB Green Premix Ex Taq II (TaKaRa, Dalian, China) as required by the protocol. The level was quantified after normalization with glyceraldehyde-3-phosphate dehydrogenase (GAPDH; for XIST and STX17) and U6 (for miR-361-3p) via the $2^{-\Delta\Delta Ct}$ method. Primer information was listed: XIST (Forward: 5'-CTTAAAGCGCTGCAATTCGCT-3', Reverse: 5'-AGGGTGTTGGGGGACTAGAA-3'); miR-361-3p (Forward: 5'-ACACTCCAGCT-GGGTCCCCCAGGTGTGATTC-3', Reverse: 5'-CTCAACTGGTGTCGTGGAGTCGGCAAT-TCAGTTGAGAAATCAGA-3'); STX17 (Forward: 5'-CCAGCCAAACTGACAAGAAA-3', Reverse: 5'-ACACCCCAGCAAACAACAA-3'); GAPDH (Forward: 5'-ACTCCTCCACCTTT-

GACGC-3', Reverse: 5'-GCTGTAGCCAAAT-TCGTTGTC-3'). U6 (Forward: 5'-CTCGCTTC-GGCAGCACA-3', Reverse: 5'-AACGCTTCAC-GAATTTGCGT-3').

3-(4,5-Dimethyl-2-Thiazolyl)-2,5-Diphenyl-2-H-Tetrazolium Bromide (MTT) Assay

The treated RB cells were harvested in a centrifuge tube, and then, seeded in a 96-well plate with a density of 2×10^3 cells/well. Subsequently, the cells were cultured for 24 h, 48 h, or 72 h, 20 μL MTT reagent (Sigma-Aldrich, St. Louis, MO, USA) was added into each well and continuously incubated for another 4 h at 37°C. After the abandonment of the medium, 150 μL of dimethyl sulfoxide (DMSO; Sigma-Aldrich) was supplemented to dissolve the generated sediment. The optical density value was estimated using a microplate reader at 490 nm.

Flow Cytometry Assay

For cell apoptosis assay, Annexin V-fluorescein isothiocyanate (FITC)/propidium iodide (PI) Apoptosis Kit (Solarbio, Beijing, China) was employed. Firstly, the treated cells were re-suspended in the binding buffer, and then Annexin V-FITC and PI were supplemented into the cell suspension. After double stain, the apoptotic cells were distinguished and analyzed using a FACS-Calibur (BD Biosciences, Franklin Lakes, NJ, USA).

Transwell Assay

For cell migration assay, Y79 and WERI-Rb-1 cells (4×10^5) in serum free-medium (200 μL) were added into the upper chamber of 24-well transwell chambers (8 μm, Corning Costar, Corning, NY, USA) at 48 h post-transfection. Simultaneously, 600 μL RPMI1640 media with 20% FBS were supplemented into the lower chamber. After incubation for 24 h, the removed cells were stained with 0.1% crystal violet (Sigma-Aldrich) and photographed. For cell invasion assay, the protocol was similar to the cell migration assay except that the upper chamber was pre-coated with Matrigel (Corning Costar) before the addition of cell suspension.

Western Blot Assay

As previously described[25], the proteins from clinical tissues and cells were segregated through adopting sodium dodecyl sulfate-polyacrylamide gels (SDS-PAGE) (12%). The isolated protein was transferred onto a polyvinylidene difluoride membranes (PVDF; Millipore, Billerica, MA, USA). After that, 5% skim milk powder was applied for blockage, and the primary antibodies (Abcam, Cambridge, MA, USA) were supplemented with the corresponding dilution. On the next day, a matched secondary antibody was added to combine the formed complex, and unique protein was captured and appeared with the help of an enhanced chemiluminescence reagent (Millipore, Billerica, MA, USA). All the primary antibodies were shown: anti- autophagy microtubule-associated protein light chain beta 3 (LC3B; b51520, 1:3000), anti-p62 (ab56416, 1:1000), anti-Beclin1 (ab210498, 1:1000), and anti-GAPDH (ab8245, 1:7500).

Dual-Luciferase Reporter Assay

The XIST and STX17 fragments that possessed unique miR-361-3p binding sites were subcloned into the basic vector of pmirGLO (Promega, Madison, WI, USA) to create the wildtype reporters (WT-XIST and STX17 3'UTR-WT). Similarly, the common sequences were mutated and inserted into the pmirGLO to generate mutant reporters (MUT-XIST and STX17 3'UTR-MUT). The above-formed reporters were co-transfected with Renilla vector (pRL-TK; Promega, Madison, WI, USA) into RB cells that have been treated with miR-361-3p or miR-NC, respectively. Exactly 48 h after transfection, Dual-Luciferase Assay System Kit (Promega, Madison, WI, USA) was used to measure the luciferase activity.

Xenograft Tumor Model

The nude mice were obtained from Vital River Laboratory Animal Technology (Beijing, China) and divided into two groups (n=5/group) randomly. Briefly, Y79 cells were subjected to lentivirus-mediated sh-XIST or sh-NC. After transfection for 48 h, the cells were re-suspended with 200 μL phosphate buffer solution (PBS; Gibco, Waltham, MA, USA), and then, injected into the flank of the nude mice subcutaneously. Next, tumor length and width were measured every 4 days at one-week post-injection, and the tumor volume was calculated: volume=length×width^2×0.5. After injection for 27 days, the treated nude mice were sacrificed, and the formed tumors were fetched and weighed. In addition, our experiments were ratified by the Institutional Animal Care and Use Committee of The Affiliated Hospital of Guizhou Medical University.

Statistical Analysis

All the experiments were repeated in triplicate, and the data were expressed as the mean ± standard deviation (SD). The difference between the two groups was assessed using two-tailed Student's *t*-test, and the comparison among the multiple groups was analyzed with the use of a one-way analysis of variance with the Tukey test. *p*-value less than 0.05 was regarded as statistically significant.

Results

Knockdown of XIST Promoted Cell Apoptosis, Impeded Proliferation, Migration, Invasion and Autophagy

Firstly, the expression profile of XIST was uncovered. Compared with the normal tissues, XIST was apparently overexpressed in RB tissues (Figure 1A). Interestingly, a similar tendency of XIST expression was observed in RB cells (Y79 and WERI-Rb-1) with respect to the normal cells (Figure 1B). The aberrant expression of XIST prompted us to highlight the function of XIST. As shown in Figure 2A, after transfection with si-XIST, the level of XIST was indeed declined in Y79 and WERI-Rb-1 cells compared with that of si-NC transfection. Subsequently, functional assays were performed to explore the role of XIST in cellular phenotypes. MTT analysis demonstrated that cell proliferation was clearly restrained in XIST deficient RB cells (Figure 2B and 2C). On the contrary, the absence of XIST caused a notable reinforcement of the apoptosis in the two RB cells (Figure 2D). Moreover, we explore the influence of XIST deficiency on cell mobility. As plotted in Figure 2E-2H, both

cell migration and invasion were particularly hindered in XIST-silenced Y79 and WERI-Rb-1 cells. Meanwhile, the capacity of cell autophagy was determined. After introduction with si-XIST, the ratio of LC3II/LC3I and Beclin1 level was evidently decreased, whereas p62 level was significantly upregulated *in vitro*. That was to say, loss of XIST led to the reduction of cell autophagy in the two RB cells (Figure 2I and 2J). The above evidence revealed that the ectopic expression of XIST could regulate aggression phenotypes, showing as the acceleration of cell apoptosis, and repression of cell proliferation, migration, invasion, autophagy when XIST was silenced in RB cells.

XIST Exerted Its Roles Via Sponging MiR-361-3p in RB Cells

In view of the function of XIST in RB, finding the candidate targets of XIST was the subsequent purpose of this research. As predicted by starBase, there were some binding sites between XIST and miR-361-3p (Figure 3A). Afterwards, Dual-Luciferase reporter assay was implemented to confirm the interaction between them. We displayed that miR-361-3p only impeded the Luciferase activity of WT-XIST reporter but had no significant influence on altering the luciferase activity of MUT-XIST reporter in Y79 and WERI-Rb-1 cells (Figure 3B and 3C). The results supported the conclusion that miR-361-3p was a target of XIST. Subsequently, an effective low expression of miR-361-3p was observed in RB tissues and cells in contrast to the selected controls (Figure 3D and 3E). Interestingly, the level of miR-361-3p was inversely related to XIST level in RB samples (Figure 3F). All the discoveries drove us to expound
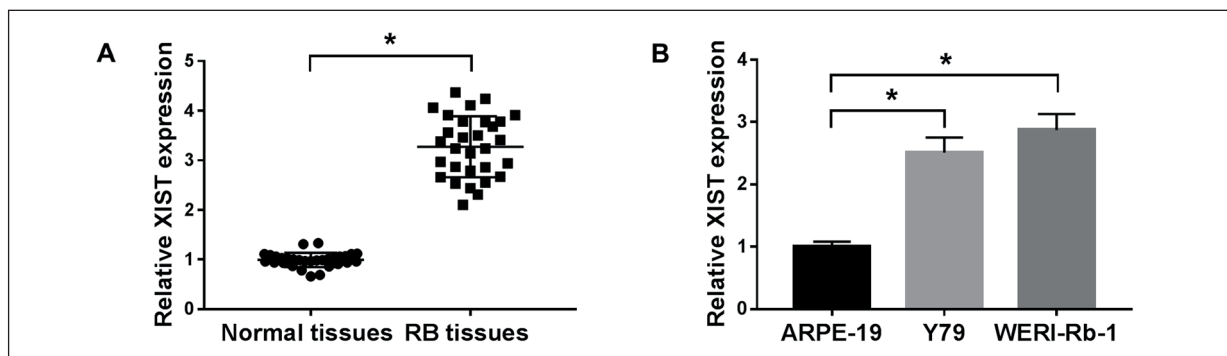

Figure 1. The level of XIST was upregulated in RB tissues and cells. **A,** and **B,** QRT-PCR analysis for the level of XIST in clinical RB tissues and selected cells (Y79 and WERI-Rb-1) with respect to relative controls (Normal tissues and ARPE-19 cells). Data are presented as mean ± SD of three independent tests. **p*<0.05.
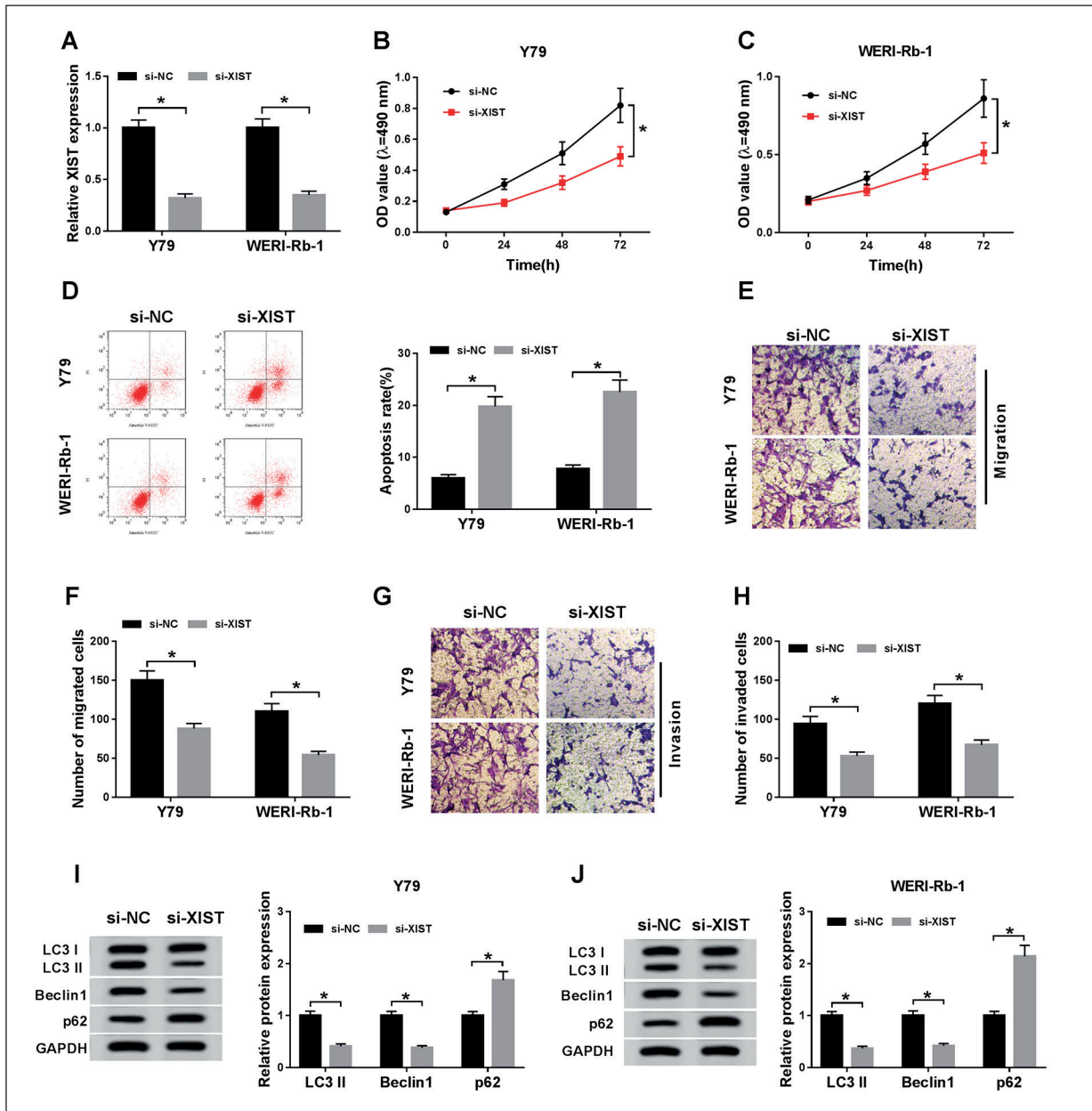
Figure 2. Knockdown of XIST promoted cell apoptosis, impeded proliferation, migration, invasion and autophagy. **A-J,** Si-XIST or si-NC was introduced into Y79 and WERI-Rb-1 cells. **A,** Relative level of XIST in si-XIST-transfected cells. **B,** and **C,** MTT analysis for the alteration of cell proliferation in the two RB cells with XIST silencing. **D,** Flow cytometry analysis for the apoptosis of Y79 and WERI-Rb-1 cells under XIST absence. **E-H,** The effect of XIST deficiency on cell migration and invasion (100x) *in vitro.* **I,** and **J,** Western blot analysis for the alteration of autophagy-related proteins (LC3I, LC3 II, Beclin1 and p62) in XIST-silenced RB cells. The data were presented as mean ± SD of three independent experiments. *$*p$<0.05.

the functional mechanism between miR-361-3p and XIST. Firstly, we validated that the absence of XIST caused a noticeable augment of the level of miR-361-3p in the two RB cells (Figure 3G). Thereafter, si-XIST alone or along with anti-miR-361-3p was transfected into Y79 and WERI-Rb-1 cells; the high level of miR-361-3p caused by XIST detection was notably decreased *in vitro* (Figure 3H). Next, rescue assays about cell behaviors were carried out. As depicted in Figure 3I and 3J, the reintroduction of miR-361-3p inhibitor could overturn XIST deficiency-mediated repression of cell proliferation in selected RB cells. In addition, cell apoptosis
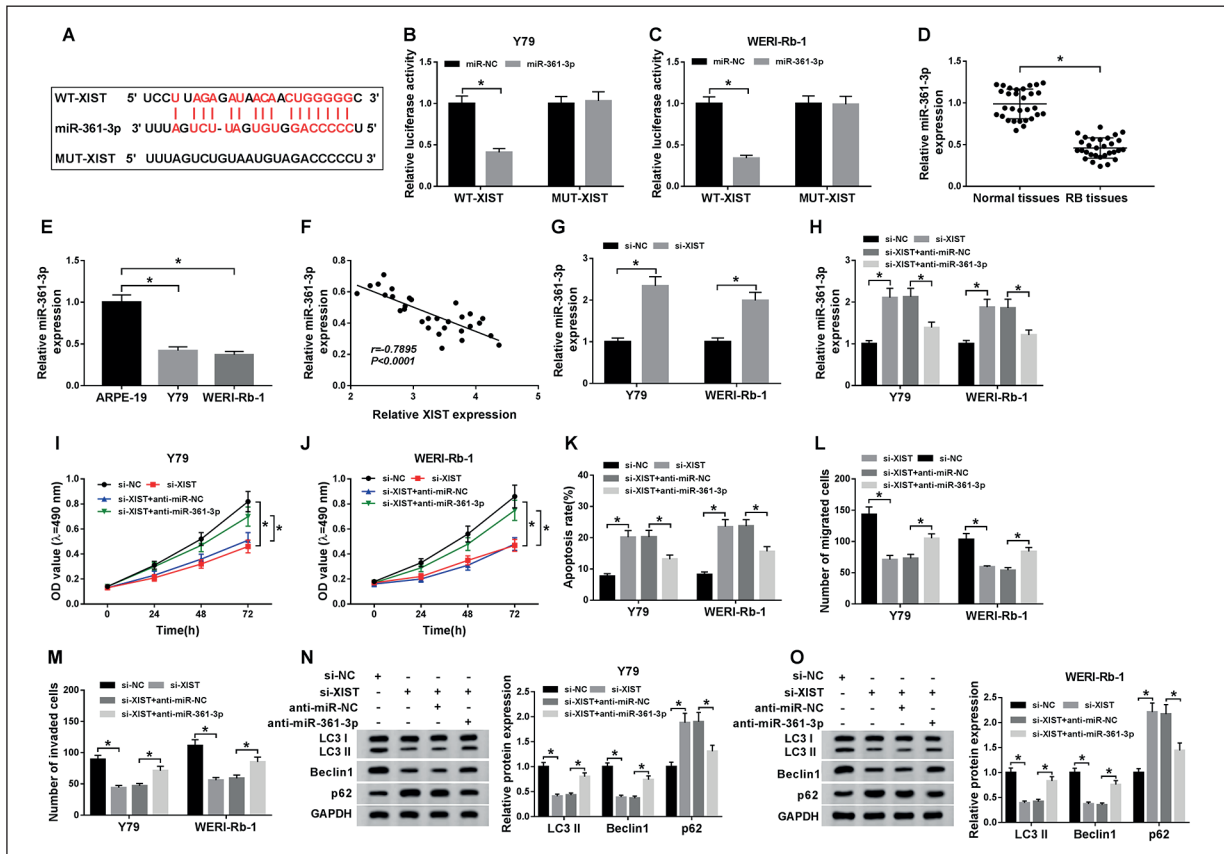
Figure 3. XIST exerted its roles *via* sponging miR-361-3p in RB cells. **A,** The common fragments between XIST and miR-361-3p. **B,** and **C,** Dual-Luciferase reporter analysis for verifying the relationship between miR-361-3p and XIST in the two RB cells. **D,** and **E,** Relative level of miR-361-3p in RB tissues and cells compared with matched controls. **F,** Correlation between miR-361-3p and XIST in clinical RB tissues. **G,** QRT-PCR analysis for the influence of XIST detection on the level of miR-361-3p in RB cells. **H-O,** Si-NC, si-XIST, si-XIST+anti-miR-NC, or si-XIST+anti-miR-361-3p was transfected into Y79 and WERI-Rb-1 cells. **H,** The impact of si-XIST and anti-miR-361-3p transfection on the level of miR-361-3p *in vitro*. **I,** and **J,** The alteration of cell proliferation in Y79 and WERI-Rb-1 cells under si-XIST and anti-miR-361-3p transfection. **K,** The effect of XIST or miR-361-3p silencing on cell apoptosis in RB cells. **L,** and **M,** The capacities of the migration and invasion in si-XIST and anti-miR-361-3p-treated RB cells. **N,** and **O,** Western blot analysis for the alteration of cell autophagy of the two RB cells. Data were presented as mean ± SD of three different experiments. *$p<0.05$.

was facilitated as a result of XIST detection, and such acceleratory effect was recovered after co-transfection with anti-miR-361-3p in Y79 and WERI-Rb-1 cells (Figure 3K). Also, results from transwell assay presented that knockdown of XIST effectively retarded cell migration and invasion, but regain of miR-361-3p inhibitor could restore this impact *in vitro* (Figure 3L and 3M). Of note, the sharp decline of cell autophagy resulted from XIST silencing was markedly abolished by miR-361-3p inhibition in both Y79 and WERI-RB-1 cells (Figure 3M and 3O). All the findings suggested that XIST was a sponge of miR-361-3p to modulate cellular behaviors, including cell proliferation, apoptosis, migration, invasion, and autophagy, in RB cells.

STX17 Was a Direct Target of MiR-361-3p

Given the function of miR-361-3p, we further investigated the detailed targets of miR-361-3p. After prediction by starBase, miR-361-3p was partially bound to the STX17 (Figure 4A). Subsequently, we found that miR-361-3p could decrease about 60% of the Luciferase activity of STX17 3'UTR-WT reporter system, while had no significant effect on changing the luciferase activity of the matched mutant reporter in Y79 and WERI-Rb-1 cells (Figure 4B and 4C). Afterwards, efficient high expression of STX17 was observed in RB tissues and cells compared with normal tissues and cells (Figure 4D-4G). Expectantly, the level of STX17
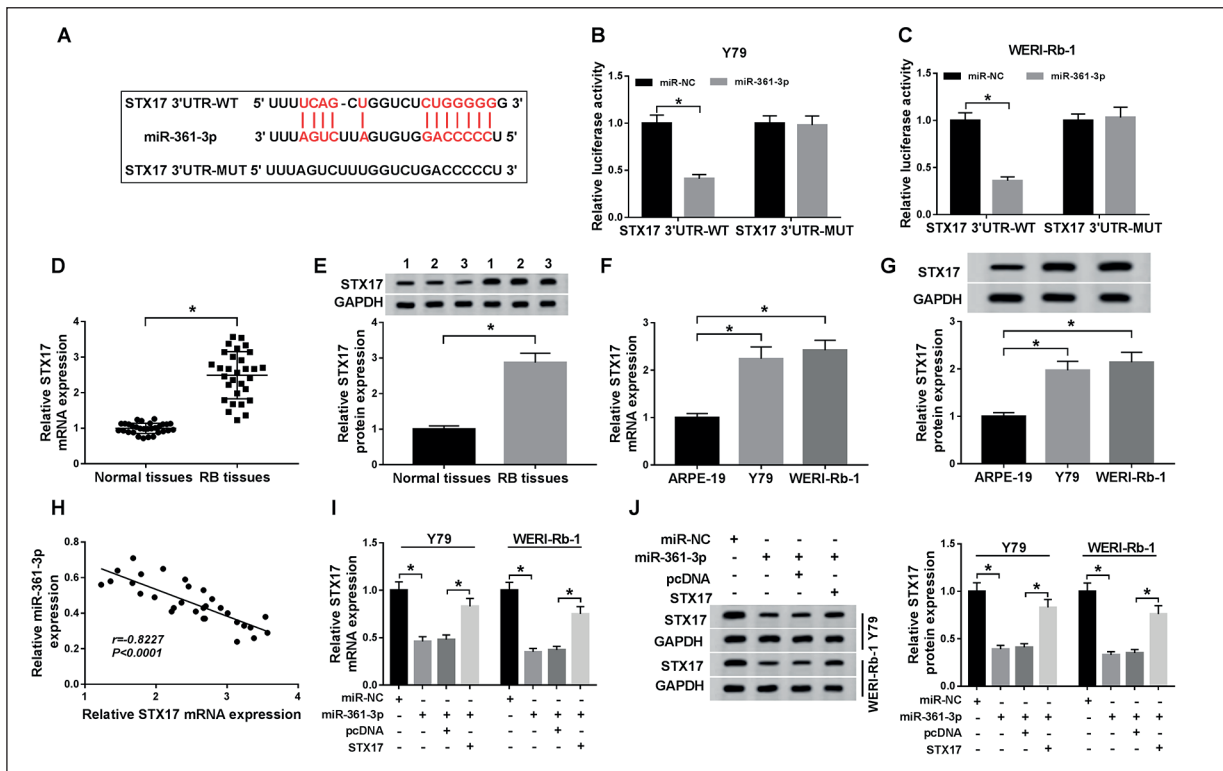
Figure 4. STX17 was a direct target of miR-361-3p. **A,** The predictive complementary binding sites between miR-361-3p and STX17. **B, and C,** Luciferase activities of STX17 3'UTR-WT and STX17 3'UTR-MUT in miR-361-3p-transfected Y79 and WERI-Rb-1 cells. **D-G,** The mRNA and protein levels of STX17 in RB tissues and cells in comparison with relative controls. **H,** Correlation between miR-361-3p level and STX17 expression in clinical RB tissues. **I, and J,** Relative level of STX17 in the two RB cells under miR-361-3p and STX17 transfection. All data were exhibited as mean ± SD, each test was repeated 3 times. *$p < 0.05$.

was passively correlated with miR-361-3p in clinical RB tissues (Figure 4H). On this basis, we aimed to discover the molecular regulation between miR-361-3p and STX17. Briefly, miR-361-3p alone or plus STX17 was transfected into Y79 and WERI-Rb-1 cells, and the mRNA and protein levels of STX17 were assayed. As plotted in Figure 4I and 4J, miR-361-3p mimic sharply blocked the level of STX17, while the reintroduction of STX17 reversed this effect in the two RB cells. These discoveries disclosed that miR-361-3p exerted its role via regulating STX17 in RB.

XIST/MiR-361-3p Axis Regulated Cell Behaviors Via STX17 in RB Cells

In view of the foregoing conclusion, the functional regulation between miR-361-3p and STX17 was the purpose of this study. Firstly, miR-361-3p alone or combined with STX17 was introduced into Y79 and WERI-Rb-1 cells, and MTT analysis demonstrated that the regain of

STX17 could revert the repressive influence of miR-361-3p on cell proliferation *in vitro* (Figure 5A and 5B). Simultaneously, cell apoptosis was apparently enhanced in miR-361-3p-mediated RB cells, and STK17 supplement could abrogate this impact (Figure 5C). Also, transwell analysis exhibited that the low ability of cell mobility, resulted from miR-361-3p increase, was substantially expedited after reintroduction with STX17 in Y79 and WERI-Rb-1 cells (Figure 5D and 5E). Besides, we also determined the protein levels of LC3II/LC3I, Beclin1 and p62 in response to the ectopic levels of miR-361-3p and STX17, and concluded that STX17 upregulation obviously eliminated miR-361-3p-mediated reductive impact on cell autophagy *in vitro* (Figure 5F-5I). Based on this, we systemically explored the regulatory mechanism between miR-361-3p and XIST or STX17 in RB cells. After transfection with si-XIST alone or plus anti-miR-361-3p in the two RB cells, qRT-PCR and Western blot as-
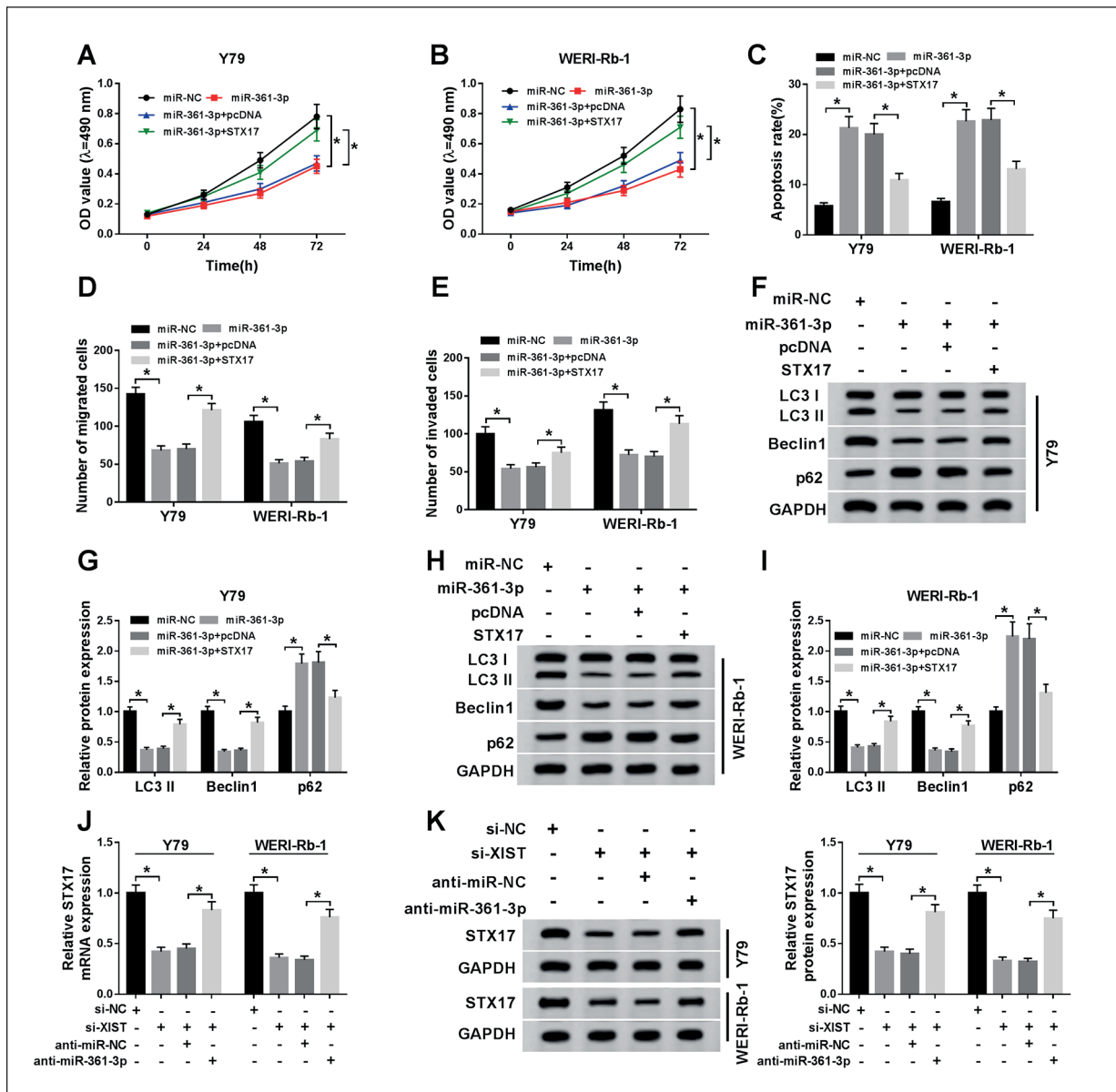
Figure 5. XIST/miR-361-3p axis regulated cell behaviors via STX17 in RB cells. **A-K,** Y79 and WERI-Rb-1 cells were transfected with miR-NC, miR-361-3p, miR-361-3p+pcDNA, or miR-361-3p+STX17, respectively. **A,** and **B,** The proliferation of the two RB cells treated accordingly. (C) The influence of miR-361-3p and STX17 on cell apoptosis *in vitro*. **D,** and **E,** Transwell analysis for the ability of cell migration and invasion in miR-361-3p and STX17-transfected cells. **F-I,** The impact miR-361-3p and STX17 on cell autophagy via measuring the level of relative proteins in RB cells. **J,** and **K,** Relative level of STX17 in Y79 and WERI-Rb-1 after transfection with si-XIST or anti-miR-361-3p. Data were represented as mean ± SD, and each experiment was repeated 3 times. *$p<0.05$.

says were conducted to determine the mRNA and protein levels of STX17, respectively. The results illustrated that the level of STX17 was diminished as a result of XIST detection, and such curb effect could be relieved *via* synchronous transfection with miR-361-3p inhibitor in Y79 and WERI-Rb-1 cells (Figure 5J and 5K).

In brief, XIST functioned its oncogenic role via miR-361-3p/STX17 axis in RB progression.

XIST Diminished Tumor Growth In Vivo

As mentioned above, we further focused on the function of XIST in tumor growth *in vivo*. In this assay, lentivirus-mediated Y79 cells (sh-

XIST or sh-NC) were injected into the grouped nude mice, and sh-XIST-treatment could significantly retard tumor volume and weight in excised tumors (Figure 6A and 6B). Then, the levels of XIST and miR-361-3p were reckoned using qRT-PCR assay. The results exhibited that XIST was forcefully hampered, but miR-361-3p was distinctly upregulated in sh-XIST-injected group (Figure 6C). Furthermore, the mRNA and protein levels of STX17 were measured. As grafted in Figure 6D and 6E, a statistical decline of STX17 level was observed when XIST was silenced in xenograft tumor specimens. Collectively, XIST could suppress tumor growth *via* miR-361-3p/STX17 axis *in vivo*.

Discussion

RB is intraocular cancer, commonly diagnosed among children[6,26]. Despite the emergence of several therapeutic strategies for RB, novel biological therapies, including targeted molecular therapies, remain required because of the unsatisfactory treatments of current therapies, such as unneglectable toxicity and adverse reactions. Many factors, such as age and gender, affect the occurrence and progression of RB, whereas genetic changes are the master determinants in process[27].

Up to date, lncRNAs and miRNAs have been corroborated to be connected with the initiation and development of various neoplasm, concerning their impact on the targeted molecules[28]. Besides, lncRNAs were regarded to penetrate into various aspects of gene modulation, such as epigenetic inheritance, post-transcription, and translation[29]. For instance, Actin filament-associated protein 1 antisense RNA 1 (AFAP1-AS1) is elevated in RB tissues and is closely associated with tumor growth and optic nerve invasion[30]. Alternatively, Metastasis Associated Lung Adenocarcinoma Transcript 1 (MALAT1) regulated cell autophagy through acting on miR-124 in RB cells[31]. XIST is a well-identified lncRNA in several human tumors, such as hepatocellular carcinoma[32] and prostate cancer[16]. Surprisingly, XIST acted as the opposite function in diverse cancers. In RB, XIST has been reported to promote the pathogenesis and tumorigenesis. The absence of XIST could hinder cell proliferation in RB cells[33]. In the current investigation, the high expression statue of XIST in RB was particularly confirmed in RB tissues and cells (Y79 and WERI-Rb-1). Furthermore, functional assays were administrated in XIST-silenced RB
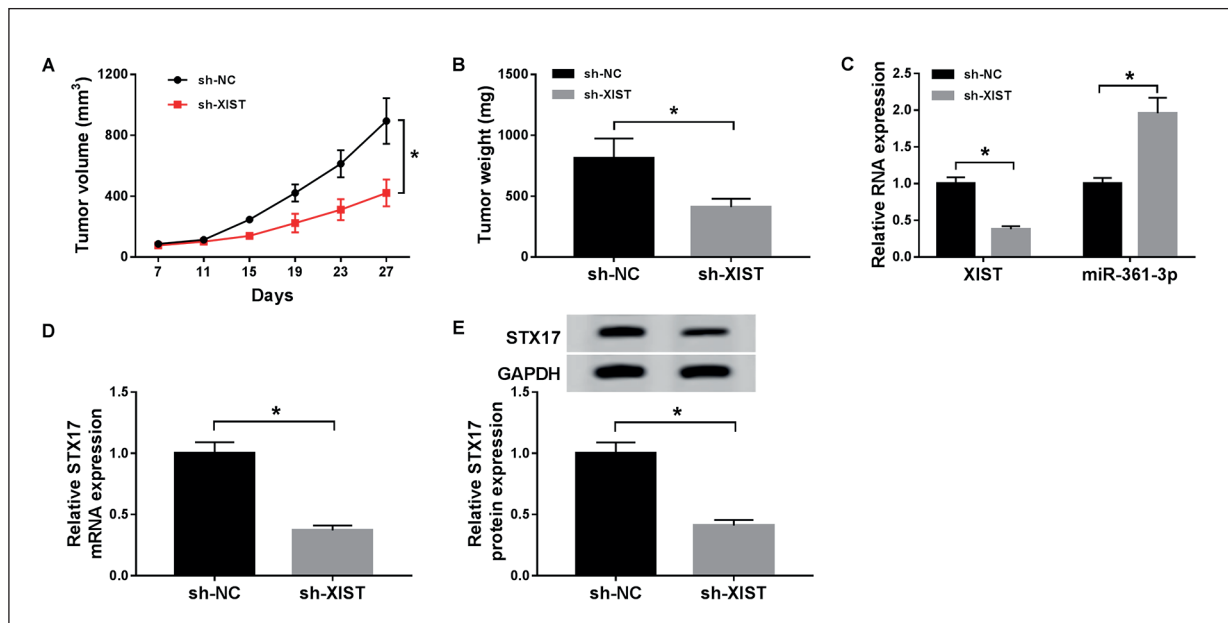

Figure 6. XIST diminished tumor growth *in vivo*. **A,** and **B,** The volume and weight of the excised tumors after treatment with sh-XIST or sh-NC. **C,** Relative levels of XIST and miR-361-3p in xenograft tumors. **D,** and **E,** The mRNA and protein levels of STX17 in lentivirus-mediated tissues. Data were expressed as means ± SD of three independent assays. *$p<0.05$.

cells, and we found that XIST detection led to the suppression of cell proliferation, migration, invasion, autophagy, and promotion of apoptosis in selected RB cells. Moreover, the oncogenic role of XIST in RB was also elucidated in the xenograft tumor model.

Of note, lncRNAs could act as ceRNAs to affect miRNA expression, thereby influencing the actions of targeted miRNA[34]. Previous studies[17,35] clarified the interactions between XIST and miRNAs in carcinogenesis. To be specific, XIST was a sponge of miR-101 to regulate gastric cancer development and RB. Therefore, we aimed to seek the special targets of XIST. According to the prediction of starBase software, we discovered that miR-361-3p was one of the possible targets. In general, miRNAs participate in the pathogenesis and tumorigenesis. For example, miR-125b was notably augmented in RB cells, triggering tumor growth and hampering cell apoptosis[36]. For miR-361-3p, it was tightly associated with human cancers. Hu et al[37] demonstrated that microRNA-361-3p acted as an oncogene in pancreatic ductal adenocarcinoma, and upregulation of miR-361-3p could promote cell mobility *in vitro*. However, the level of miR-361-3p was distinctly decreased in RB tissues and cells and served as a tumor-suppressive miRNA in human RB[22]. The above introduction meant that the function of miR-361-3p was inconsistent in different organs. In this present paper, a low expression of miR-361-3p was observed in RB tissues and cells, which was agreed with a previous research[22]. On this basis, the functional mechanism between miR-361-3p and XIST was analyzed, and we manifested that miR-361-3p could eliminate the impact of XIST silencing on cell proliferation, apoptosis, migration, invasion, and autophagy *in vitro*.

Over the past decades, STX17 has been proved to be an autophagy-related factor[38]. The loss of STX17 resulted in the accumulation of autophagosomes without degradation[39]. We focused on the role of STX17 in altering cell phenotypes in RB cells. Firstly, we found that STX17 was a potential target of miR-361-3p. Huang et al[31] implied that STX17 was targeted by miR-124 to modulate cell autophagy of RB cells. Also, STX17 could revert miR-361-3p mimic-mediated reductive influence on cell autophagy in the two RB cells. Not only that, the upregulation of STX17 eliminated the impact of miR-361-3p supplement on cell proliferation, apoptosis, migration, and invasion *in vitro*. We concluded that STX17, as a target of

miR-361-3p, went in for the onset and progression of human RB.

Conclusions

Conclusively, this current study manifested that highly expressed XIST could reinforce the progression and aggravation of RB by miR-361-3p/STX17 axis, providing strong evidence for exploring potential diagnostic and therapeutic biomarkers for RB. Nevertheless, further experiments are needed to investigate the consequences of this research.

Conflict of Interest

The Authors declare that they have no conflict of interests.

References

1) SHIELDS CL, SHIELDS JA. Retinoblastoma management: advances in enucleation, intravenous chemoreduction, and intra-arterial chemotherapy. Curr Opin Ophthalmol 2010; 21: 203-212.

2) SHIELDS CL, LALLY SE, LEAHEY AM, JABBOUR PM, CAYWOOD EH, SCHWENDEMAN R, SHIELDS JA. Targeted retinoblastoma management: when to use intravenous, intra-arterial, periocular, and intravitreal chemotherapy. Curr Opin Ophthalmol 2014; 25: 374-385.

3) TURCOTTE LM, LIU Q, YASUI Y, ARNOLD MA, HAMMOND S, HOWELL RM, SMITH SA, WEATHERS RE, HENDERSON TO, GIBSON TM, LEISENRING W, ARMSTRONG GT, ROBISON LL, NEGLIA JP. Temporal trends in treatment and subsequent neoplasm risk among 5-year survivors of childhood cancer, 1970-2015. JAMA 2017; 317: 814-824.

4) GAO J, ZENG J, GUO B, HE W, CHEN J, LU F, CHEN D. Clinical presentation and treatment outcome of retinoblastoma in children of South Western China. Medicine (Baltimore) 2016; 95: e5204.

5) KALIKI S, SHIELDS CL. Retinoblastoma: achieving new standards with methods of chemotherapy. Indian J Ophthalmol 2015; 63: 103-109.

6) SHIELDS CL, MASHAYEKHI A, AU AK, CZYZ C, LEAHEY A, MEADOWS AT, SHIELDS JA. The international classification of retinoblastoma predicts chemoreduction success. Ophthalmology 2006; 113: 2276-2280.

7) ZAGE PE, REITMAN AJ, SESHADRI R, WEINSTEIN JL, METS MB, ZEID JL, GREENWALD MJ, STRAUSS LC, GOLDMAN S. Outcomes of a two-drug chemotherapy regimen for intraocular retinoblastoma. Pediatr Blood Cancer 2008; 50: 567-572.

8) CHUNG SE, SA HS, KOO HH, YOO KH, SUNG KW, HAM DI. Clinical manifestations and treatment of retinoblastoma in Korea. Br J Ophthalmol 2008; 92: 1180-1184.

9) CONKRITE K, SUNDBY M, MUKAI S, THOMSON JM, MU D, HAMMOND SM, MACPHERSON D. MiR-17~92 co-operates with RB pathway mutations to promote retinoblastoma. Genes Dev 2011; 25: 1734-1745.

10) BRAICU C, CATANA C, CALIN GA, BERINDAN-NEAGOE I. NCRNA combined therapy as future treatment option for cancer. Curr Pharm Des 2014; 20: 6565-6574.

11) ZHU H, YU J, ZHU H, GUO Y, FENG S. Identification of key lncRNAs in colorectal cancer progression based on associated protein-protein interaction analysis. World J Surg Oncol 2017; 15: 153.

12) SCHMITT AM, CHANG HY. Long noncoding RNAs in cancer pathways. Cancer Cell 2016; 29: 452-463.

13) YANG M, WEI W. Long non-coding RNAs in retinoblastoma. Pathol Res Pract 2019; 215: 152435.

14) ZHANG H, ZHONG J, BIAN Z, FANG X, PENG Y, HU Y. Long non-coding RNA CCAT1 promotes human retinoblastoma SO-RB50 and Y79 cells through negative regulation of miR-218-5p. Biomed Pharmacother 2017; 87: 683-691.

15) YANG C, WU K, WANG S, WEI G. Long non-coding RNA XIST promotes osteosarcoma progression by targeting YAP via miR-195-5p. J Cell Biochem 2018; 119: 5646-5656.

16) ZHENG R, LIN S, GUAN L, YUAN H, LIU K, LIU C, YE W, LIAO Y, JIA J, ZHANG R. Long non-coding RNA XIST inhibited breast cancer cell growth, migration, and invasion via miR-155/CDX1 axis. Biochem Biophys Res Commun 2018; 498: 1002-1008.

17) CHENG Y, CHANG Q, ZHENG B, XU J, LI H, WANG R. LncRNA XIST promotes the epithelial to mesenchymal transition of retinoblastoma via sponging miR-101. Eur J Pharmacol 2019; 843: 210-216.

18) ZHANG Y, LI Y, WANG Q, ZHANG X, WANG D, TANG HC, MENG X, DING X. Identification of an ln-cRNAmiRNAmRNA interaction mechanism in breast cancer based on bioinformatic analysis. Mol Med Rep 2017; 16: 5113-5120.

19) ZHANG Q, CHEN B, LIU P, YANG J. XIST promotes gastric cancer (GC) progression through TGF-beta1 via targeting miR-185. J Cell Biochem 2018; 119: 2787-2796.

20) MULRANE L, MCGEE SF, GALLAGHER WM, O'CONNOR DP. MiRNA dysregulation in breast cancer. Cancer Res 2013; 73: 6554-6562.

21) CHEN W, WANG J, LIU S, WANG S, CHENG Y, ZHOU W, DUAN C, ZHANG C. MicroRNA-361-3p suppresses tumor cell proliferation and metastasis by directly targeting SH2B1 in NSCLC. J Exp Clin Cancer Res 2016; 35: 76.

22) ZHAO D, CUI Z. MicroRNA-361-3p regulates retinoblastoma cell proliferation and stemness by targeting hedgehog signaling. Exp Ther Med 2019; 17: 1154-1162.

23) LYTLE JR, YARIO TA, STEITZ JA. Target mRNAs are repressed as efficiently by microRNA-binding sites in the 5' UTR as in the 3' UTR. Proc Natl Acad Sci U S A 2007; 104: 9667-9672.

24) HAMASAKI M, FURUTA N, MATSUDA A, NEZU A, YAMAMOTO A, FUJITA N, OOMORI H, NODA T, HARAGUCHI T, HIRAOKA Y, AMANO A, YOSHIMORI T. Autophago-somes form at ER-mitochondria contact sites. Nature 2013; 495: 389-393.

25) ZHENG J, LIU X, WANG P, XUE Y, MA J, QU C, LIU Y. CRNDE promotes malignant progression of glioma by attenuating miR-384/PIWIL4/STAT3 axis. Mol Ther 2016; 24: 1199-1215.

26) VILLEGAS VM, HESS DJ, WILDNER A, GOLD AS, MURRAY TG. Retinoblastoma. Curr Opin Ophthalmol 2013; 24: 581-588.

27) CINTI C, CLAUDIO PP, HOWARD CM, NERI LM, FU Y, LEONCINI L, TOSI GM, MARALDI NM, GIORDANO A. Genetic alterations disrupting the nuclear localization of the retinoblastoma-related gene RB2/p130 in human tumor cell lines and primary tumors. Cancer Res 2000; 60: 383-389.

28) GARZON R, MARCUCCI G, CROCE CM. Targeting microRNAs in cancer: rationale, strategies and challenges. Nat Rev Drug Discov 2010; 9: 775-789.

29) HUANG X, XIAO R, PAN S, YANG X, YUAN W, TU Z, XU M, ZHU Y, YIN Q, WU Y, HU W, SHAO L, XIONG J, ZHANG Q. Uncovering the roles of long non-coding RNAs in cancer stem cells. J Hematol Oncol 2017; 10: 62.

30) HAO F, MOU Y, ZHANG L, WANG S, YANG Y. Ln-cRNA AFAP1-AS1 is a prognostic biomarker and serves as oncogenic role in retinoblastoma. Biosci Rep 2018; 38.

31) HUANG J, YANG Y, FANG F, LIU K. MALAT1 modulates the autophagy of retinoblastoma cell through miR-124-mediated stx17 regulation. J Cell Biochem 2018; 119: 3853-3863.

32) CHANG S, CHEN B, WANG X, WU K, SUN Y. Long non-coding RNA XIST regulates PTEN expression by sponging miR-181a and promotes hepatocellular carcinoma progression. BMC Cancer 2017; 17: 248.

33) HU C, LIU S, HAN M, WANG Y, XU C. Knockdown of lncRNA XIST inhibits retinoblastoma progression by modulating the miR-124/STAT3 axis. Biomed Pharmacother 2018; 107: 547-554.

34) KALLEN AN, ZHOU XB, XU J, QIAO C, MA J, YAN L, LU L, LIU C, YI JS, ZHANG H, MIN W, BENNETT AM, GREGORY RI, DING Y, HUANG Y. The imprinted H19 lncRNA antagonizes let-7 microRNAs. Mol Cell 2013; 52: 101-112.

35) CHEN DL, JU HQ, LU YX, CHEN LZ, ZENG ZL, ZHANG DS, LUO HY, WANG F, QIU MZ, WANG DS, XU DZ, ZHOU ZW, PELICANO H, HUANG P, XIE D, WANG FH, LI YH, XU RH. Long non-coding RNA XIST regulates gastric cancer progression by acting as a molecular sponge of miR-101 to modulate EZH2 expression. J Exp Clin Cancer Res 2016; 35: 142.

36) BAI S, TIAN B, LI A, YAO Q, ZHANG G, LI F. MicroR-NA-125b promotes tumor growth and suppresses apoptosis by targeting DRAM2 in retinoblastoma. Eye (Lond) 2016; 30: 1630-1638.

37) HU J, LI L, CHEN H, ZHANG G, LIU H, KONG R, CHEN H, WANG Y, LI Y, TIAN F, LV X, LI G, SUN B. MiR-361-3p regulates ERK1/2-induced EMT via DUSP2 mRNA degradation in pancreatic ductal adenocarcinoma. Cell Death Dis 2018; 9: 807.

38) ONORATI AV, DYCZYNSKI M, OJHA R, AMARAVADI RK. Targeting autophagy in cancer. Cancer 2018; 124: 3307-3318.

39) ITAKURA E, MIZUSHIMA N. Syntaxin 17: the autophagosomal SNARE. Autophagy 2013; 9: 917-919.